

A Statistical Uncertainty Assessment on a LOFT L2-5 LBLOCA PCT Based on ACE-RSM

Kwang-II Ahn^a, Bub-Dong Chung^b, John C. Lee^c

^a*Integrated Safety Assessment, KAERI, Daejeon, Korea, kiahn@kaeri.re.kr*

^b*Thermal-Hydraulic Safety Research Division, KAERI, Daejeon, Korea*

^c*Dept. of Nuclear Engineering & Radiological Science, Univ. of Michigan, Ann Arbor, MI, USA*

Keywords: LBLOCA, PCT, Uncertainty Analysis, Optimal Algorithm, ACE-RSM.

1 ABSTRACT

When a long run time is taken to obtain the relevant output values in a complex physical model (or code), the number of statistical samples which must be evaluated through it is a critical factor in a sampling-based uncertainty analysis. Two alternative methods have been utilized to avoid the problem associated with the size of these statistical samples: one is based on Wilks' formula and the other is based on the conventional nonlinear regression approach. While both approaches provide a useful means to draw a conclusion on the resultant uncertainty with a limited number of code runs, there are also the corresponding unique limitations. For example, a conclusion based on the Wilks' formula is highly affected by the sampled values themselves and the conventional regression approach requires a priori estimate on functional forms of a regression model. Main objective of this paper is to introduce a complementary method (based on the ACE algorithm) to the Wilks' formula and the conventional regression approach for uncertainty analysis and to provide an example application to the OECD BEMUSE Phase III LOFT L2-5 LBLOCA uncertainty analysis.

2 INTRODUCTION

All participants of the OECD BEMUSE Phase-III program [Crecy et al., 2007] utilize the increased number of samples in their uncertainty quantification on the LOFT L2-5 LBLOCA than one required in the first order of Wilks' formula (i.e., 59) [Wilks, 1941; Nutt et al., 2004]. This was mainly due to one of the observations at the end of BEMUSE-II that the number of code runs should be increased instead of 59 runs that were utilized as a reference case to reduce the dispersion of the uncertainty. Like this, a concern often expressed about a sampling-based uncertainty analysis is to determine the number of samples so that model evaluations will make the cost of the analysis prohibitive. If a statistical meaning could be obtained from the results or an effective uncertainty analysis is possible from them, it is better to reduce a large sample size analysis from the aspect of cost.

From the point of view, the response surface model (RSM) [Sacks et al., 1989] has been used to give an appropriate surrogate model to an original model, by using some use of statistical designs (or a limited number of statistical samples) over all possible ranges of inputs, regression techniques, and optimization methods. This approach is very useful when it takes a long time for code run to obtain the relevant output values (such as a physical trend of performance parameter in a complex physical model) and thus the number of evaluations through it is limited to at most several tens or hundreds. The resultant model is a simple and high speed alternative model that can describe best the trend of the relevant output variable with the specified inputs. Since the functional form of the RSM is generally not known for many cases, it requires a tedious and time-consuming process to obtain the most relevant functional form between input and output parameters (coupled with multivariate nonlinear regression analysis).

The above limitation involved in the traditional RSM approach can be greatly reduced by employing the alternating conditional expectation (ACE) method [Cleveland, 1979; Breiman et al., 1985; Wang et al., 2005]. The ACE method is a generalized regression algorithm that yields an optimal relationship between a dependent variable and multiple independent variables, by maximizing the statistical correlation between the transformed dependent variable and the sum of transformed independent variables. This fundamental feature of the ACE algorithm requires an iterative convergence to the transformations for independent and

dependent variables while it does not require a priori estimate of the functional forms of transformed variables. Once the optimal transformations are obtained, a simple regression analysis can be performed to determine the functional forms for the transformed dependent and independent variables. Thus, the ACE method offers two distinctive advantages over the traditional nonlinear regression analysis. First, while nonlinear regression analysis requires a priori estimate of functional forms and in general sufficiently accurate estimates of the fitting coefficients to arrive at a converged solution, the ACE algorithm guarantees the convergence of the transformations, and, once the ACE iteration is converged, a simple regression analysis usually suffices to generate actual analytical functional forms for the transformed variables. Second, the ACE algorithm cannot produce a worse fit than the traditional RSM, because if no transformations are found to be necessary, then ACE would simply suggest nearly linear transformations for all the variables, indicating at least equal or much greater data fitting than the traditional RSM. Even though those advantages of the ACE algorithm, its practical use has been very limited in the field of thermal-hydraulic uncertainty analysis [Glaeser, 2000, IAEA, 2008].

Main objective of this paper is to introduce a complementary method (based on the ACE algorithm) to the Wilks' formula and the conventional regression approach for uncertainty analysis and to provide an example application as a complementary work to the OECD BEMUSE Phase III LOFT L2-5 LBLOCA uncertainty analysis.

3 BRIEF SUMMARY OF THE ACE ALGORITHM

For a dependent variable Y and multiple independent variables ($X_i, i = 1, \dots, p$), the objective of the ACE algorithm [Cleveland, 1979; Breiman et al., 1985; Wang et al., 2005] is to find optimal transformations $\theta(Y)$ and $\phi_i(X_i)$ that maximize the statistical correlation between $\theta(Y)$ and $\sum_i^p \phi_i(X_i)$, by treating each value of the transformed variable $\theta(Y)$ as the expectation of several realizations of the sum of transformed independent variables $\sum_i^p \phi_i(X_i)$. The resulting ACE regression model can be expressed as:

$$\theta(Y) = \alpha + \sum_{i=1}^p \phi_i(X_i) + \varepsilon \quad (1)$$

Thus, the ACE model replaces the problem of estimating a linear function of a p -dimensional variable $\mathbf{X}=(X_1, X_2, \dots, X_p)$ by estimating p separate one-dimensional functions, $\phi_i(X_i)$, and $\theta(Y)$ using an iterative method. These transformations are achieved by minimizing the unexplained variance of a linear relationship between the transformed response variable $\theta(Y)$ and the sum of transformed independent variables $\sum_i^p \phi_i(X_i)$. The error variance ε^2 that is not explained by the regression (under the constraint, $E[\theta^2(Y)] = 1$)

$$\varepsilon^2(\theta, \phi_1, \phi_2, \dots, \phi_p) = E[\theta(Y) - \sum_{i=1}^p \phi_i(X_i)]^2 \quad (2)$$

The minimization of ε^2 with respect to $\phi_1(X_1), \phi_2(X_2), \dots, \phi_p(X_p)$ and $\theta(Y)$ is carried out through a series of single-function minimization, involving the following conditional expectation and minimization

$$\phi_i(X_i) = E[\theta(Y) - \sum_{j \neq i}^p \phi_j(X_j) | X_i]^2 \quad (3a)$$

$$\theta(Y) = \frac{E[\sum_{i=1}^p \phi_i(X_i) | Y]}{\|E[\sum_{i=1}^p \phi_i(X_i) | Y]\|} \quad (3b)$$

On The final $\phi_i(X_i)$ and $\theta(Y)$ after the minimization are estimates of the optimal transformations $\phi_i^*(X_i)$ and $\theta^*(Y)$, leading to the following relationship

$$\theta^*(Y) = \sum_{i=1}^p \phi_i^*(X_i) + \varepsilon^* \quad (4)$$

where ε^* is the error that is not captured by the use of the ACE transformations and is assumed to have a normal distribution with zero mean. The minimum regression error, ε^* and maximum multiple correlation coefficient, ρ^* are related by $\varepsilon^{*2} = 1 - \rho^{*2}$. On the other hand, the minimization of ε^2 cannot be obtained directly because Eqs.(3a) and (3b) are coupled to each other. Thus, the ACE algorithm necessitates an

iterative use of the two smoothing operations of Eqs.(3) in alternating directions to obtain transformed independent and dependent variables. When a convergence is attained with an iterative scheme, the data in each transformed variable are usually smooth and slowly varying. Then, selecting simple functional forms for the transformations and performing standard regression analysis for each transformation, we can obtain the final functional form of Y versus X_1, \dots, X_p if $\theta^*(Y)$ has an inverse function: $Y = \theta^{*-1}[\sum_{i=1}^p \phi_i^*(X_i)]$.

On the other hand, the error in Eq.(2) could vanish with a judicious choice of $\theta(y)$, if $\theta(y_j)$ equals $\phi_i(x_{i,j})$ for every point of a set of N data $\{(x_{i,j}, y_j), j = 1, 2, \dots, N\}$. In practice, however, this idealized situation does not occur because the data contain a greater or lesser randomness and so do $\theta(y_j)$ and $\phi_i(x_{i,j})$. Thus, $\theta(y_j)$ is considered, in the ACE algorithm, the expectation of several realizations of $\phi_i(x_i)$ for the j 'th point, rather than a single unique realization $\phi_i(x_{i,j})$ as in conventional regression analysis. In most regression problems, there is usually only one value y_j , and hence one value $\phi_i(x_{i,j})$, for the j 'th data point, and the conditional expectation $\theta(y_j)$ has to be evaluated with the neighboring values $\{\phi_i(x_{i,k}), k = j - M, \dots, j + M\}$, for some M , treated as realizations of $\phi_i(x_{i,j})$ for the j 'th data point. Thus, data smoothing operation over the dependent and independent variables plays a primary role in the ACE algorithm.

4 MARS SIMULATION FOR THE PCT UNCERTAINTY ANALYSIS

The sampling-based method [Helton et al., 2002] has been required to quantify the overall uncertainty employed in the MARS codes by means of a statistical analysis [Chung, 2005]. In order to assess the PCT uncertainty for a LBLOCA blowdown phase, first, 14 uncertainty parameters have been chosen as a result of Phenomena Identification and Ranking Table (PIRT) on LBLOCA. As given in Table 1, the chosen parameters cover (a) physical models employed in the code and (b) initial and boundary conditions for the LBLOCA simulation. The state of knowledge about all uncertain parameters has been described by ranges and subjective probability distribution (also see Table 1). Second, the random variance of each uncertain parameter was determined by a crude Monte Carlo sampling method according to the combined probability distribution of the uncertain parameters. For uniform distribution, the minimum and maximum values are boundaries of sampling. For normal distribution, the sampling boundaries were truncated at mean $\pm 2\sigma$. Any dependency between parameters was not considered in the sampling process. Then, the MARS code calculations have been performed with sampled sets of parameters. In order to limit the number of samples for the MARS code calculations to a reasonable level, a set of 93 samples have been required to apply Wilks' formula in unilateral at the 2nd order (for 95% tolerance limit and 95% confidence interval of the code results), but 100 samples were sampled to get sufficient calculation numbers to cover the unexpected run errors. Finally, multiple input decks (each input deck has 100 samples) have been implemented to identify the effect of different sets of random samples on the PCT value, consequently resulting in several thousands of PCT values for its statistical analysis. The short transient time (i.e., 100 second in case of LOFT L2-5) enabled to perform the multiple sets of these 100 cases.

During the calculation, the ratio of the failed runs (i.e., crash of the simulation code) was 7% (i.e., 7 out of 100 runs were failed). The failure was random and its reasons were not known (maybe due to a combination of physically unreasonable random values). The failed calculations were discarded manually. The remaining outputs are the final result of the propagation of input uncertainties through the specified number of code calculations.

Table 1. MARS input parameters for PCT uncertainty analysis

| x_i | Independent parameters and their ranges: $\pm 2\sigma$ (or min/max) | | PDFs |
|-------|---|--------------|--------|
| 1 | Liquid heat transfer | $\pm 20\%$ | Normal |
| 2 | Nucleate boiling heat transfer | $\pm 23.2\%$ | Normal |
| 3 | AECL lookup CHF table | $\pm 74\%$ | Normal |
| 4 | Transition boiling | $\pm 32\%$ | Normal |
| 5 | Film boiling heat transfer | $\pm 36\%$ | Normal |
| 6 | Vapor heat transfer | $\pm 20\%$ | Normal |

| | | | |
|----|-------------------------------|-----------|---------|
| 7 | Peaking factor(Fq) | ± 14.96% | Normal |
| 8 | Cold gap size | ± 20.98mm | Uniform |
| 9 | Gap conductance | ± 80% | Uniform |
| 10 | Fuel conductivity | ± 10% | Normal |
| 11 | Decay heat | ± 6.6% | Normal |
| 12 | Break area ratio | 0.7~1.15 | Uniform |
| 13 | Pump two-phase performance | 0.0~1.0 | Uniform |
| 14 | Downcomer lateral loss coeff. | 0.0~1.0 | Uniform |

5 FORMULATION OF ACE-RSM MODELS AND THEIR RESULTS

Based on the MARS input x_i ($p=14$) and output values for the PCT (y) uncertainty analysis, the corresponding ACE-RSM models can be formulated through the following procedures:

(Step-1): Derive two types of the ACE-transformed functional forms for independent and dependent variables with the prepared N sample input and output values: $x_i \sim \hat{\phi}_i(x_i)$ and $y \sim \hat{\theta}(y)$.

(Step-2): Perform a (piece-wise) linear regression between the transformed variables, $\hat{\phi}_i(x_i)$ and $\hat{\theta}(y)$:

$$\hat{\theta}^*(y) = \alpha_0 + \sum_{i=1}^{p=14} \alpha_i \hat{\phi}_i^*(x_i). \quad (5)$$

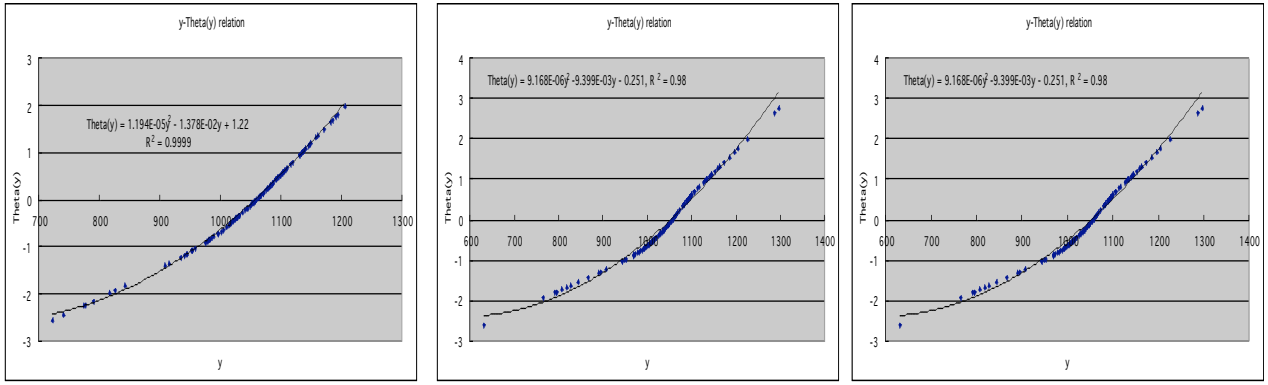
Here, it should be noted that when a convergence is well attained with an iterative scheme, a regression of the transformed dependent variable on all the transformed covariates results in all parameter coefficients of the independent variables ($\alpha_i, i = 1, 2, \dots, p$) being positive and close to 1 and the error term $\alpha_0 \approx 0$.

(Step-3): Derive the final functional form between the original input and output variables, x_i and y :

$$\hat{y} = \hat{\theta}^{*-1} \left\{ \alpha_0 + \sum_{i=1}^{p=14} \alpha_i \hat{\phi}_i^*(x_i) \right\}. \quad (6)$$

Then, 3 typical ACE-RSM models on the PCT have been formulated based on a limited number of sample runs: (a) *one from N=124 (Random Set-1): ACE-RSM-Model-1*, (b) *one from N=124 (Random Set-2): ACE-RSM-Model-2*, (c) *one from N=300: ACE-RSM-Model-3*. N=124 corresponds to the minimum number of samples required to apply the 4th order of Wilks' formula (for 95% tolerance limit and 95% confidence level of the code results), and N=300 corresponds to twice the minimum number of samples (N=153) required to apply the 4th order.

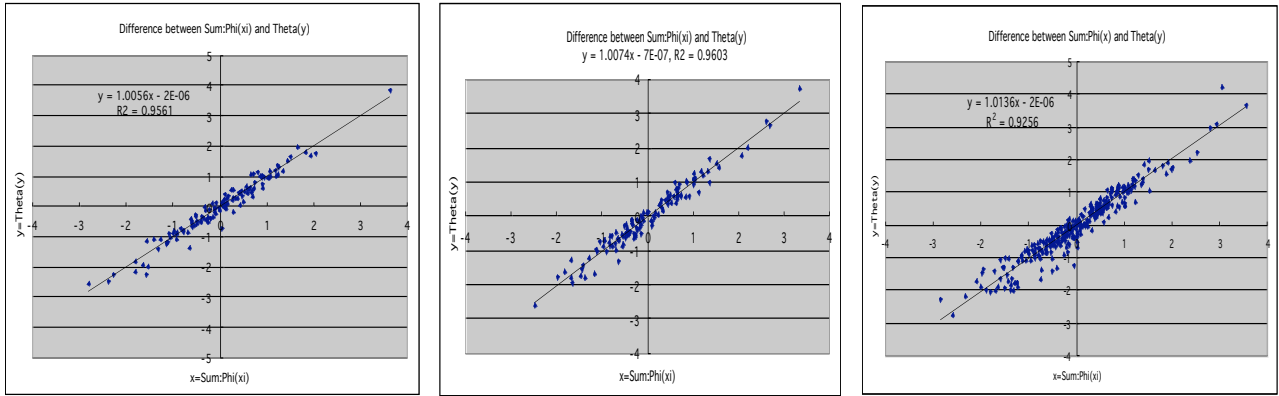
As a result of the *Step-1*, the fitted functions between x_i and $\hat{\phi}_i(x_i)$ suggested by the ACE plots have been obtained by applying the piece-wise linear or polynomial format of x_i . In addition, the fitted functions between y and $\hat{\theta}(y)$ have been obtained by applying the piece-wise linear or quadratic format of y . As a result of the *Step-2*, Figures 1-2 show functional relationships between the original output variable (y) and transformed output variable $\hat{\theta}(y)$ for the above 3 cases and between a sum of transformed inputs $\sum_{i=1}^{p=14} \hat{\phi}_i(x_i)$ and output $\hat{\theta}(y)$, respectively. Table 2 also shows the regression coefficients ($\alpha_i, i = 1, 2, \dots, p$) between $\hat{\phi}_i(x_i)$ and $\hat{\theta}(y)$. As a result of the *Step-3*, Figures 3-4 show one-to-one comparison of the ACE-RSM-based analysis results for the three ACE-RSM models with the corresponding original MARS results, with the corresponding R^2 and normalized root mean square (RMS) errors. Table 3 shows the coefficients of determination estimated from the ordinary linear regression on the original MARS simulation results. Table 4 shows 5% and 95% PCT values for the ACE-RSM models and the corresponding MARS values. Finally, Figure 5 shows a variation of the cumulative distribution function (CDF) according to the increase of sample N from 124 to 3000 in the case of ACE-RSM-1 whose form approaches the normal PDF with the increase of N.



(a) ACE-RSM-1

(b) ACE-RSM-2

(c) ACE-RSM-3

Figure 1. Functional forms of the ACE-transformed output variable $\hat{\theta}(y)$ 

(a) ACE-RSM-1

(b) ACE-RSM-2

(c) ACE-RSM-3

$$(a) \hat{\theta}^*(y) = 1.0056 \sum_{i=1}^{p=14} \hat{\phi}_i^*(x_i) - 2.0 \times 10^{-6}, R^2 = 0.96$$

$$(b) \hat{\theta}^*(y) = 1.0074 \sum_{i=1}^{p=14} \hat{\phi}_i^*(x_i) - 7.0 \times 10^{-7}, R^2 = 0.96$$

$$(c) \hat{\theta}^*(y) = 1.0136 \sum_{i=1}^{p=14} \hat{\phi}_i^*(x_i) - 2.0 \times 10^{-6}, R^2 = 0.93$$

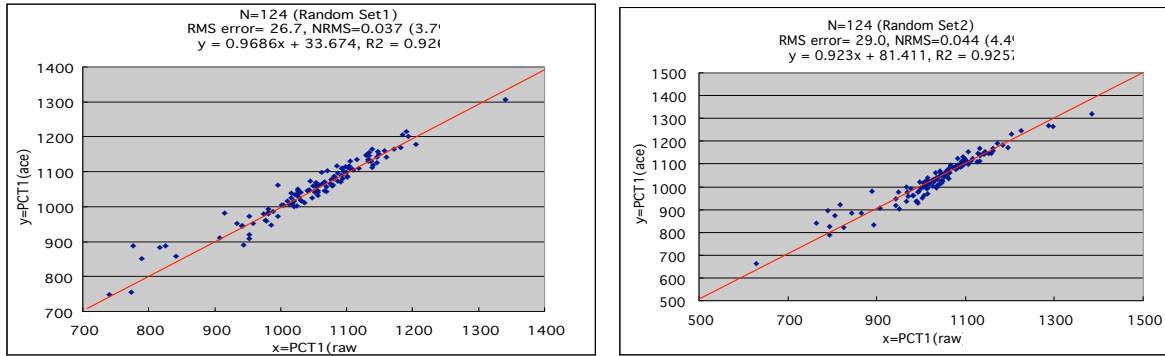
Figure 2. Relationships between the ACE-transformed inputs $\hat{\phi}_i(x_i)$ ($p=14$) and output $\hat{\theta}(y)$ **Table 2.** Regression coefficients between the ACE-transformed inputs and output.

| $\hat{\phi}^*(x_i)$ | Regression coeff. (α_i) and the square of the multiple correlation coefficient (R^2) | | |
|---------------------|---|------------------------|------------------------|
| | ACE-RSM-1 | ACE-RSM-2 | ACE-RSM-3 |
| $i=0$ | $\alpha_0 = -6.93E-07$ | $\alpha_0 = -6.93E-07$ | $\alpha_0 = -2.03E-06$ |
| $i=1$ | $\alpha_1 = 1.17$ | $\alpha_1 = 1.67$ | $\alpha_1 = 1.05$ |
| $i=2$ | $\alpha_2 = 1.08$ | $\alpha_2 = 1.39$ | $\alpha_2 = 1.50$ |
| $i=3$ | $\alpha_3 = 1.27$ | $\alpha_3 = 1.17$ | $\alpha_3 = 1.14$ |
| $i=4$ | $\alpha_4 = 1.08$ | $\alpha_4 = 0.909$ | $\alpha_4 = 1.01$ |
| $i=5$ | $\alpha_5 = 1.18$ | $\alpha_5 = 1.04$ | $\alpha_5 = 0.987$ |
| $i=6$ | $\alpha_6 = 1.21$ | $\alpha_6 = 1.48$ | $\alpha_6 = 1.17$ |
| $i=7$ | $\alpha_7 = 1.00$ | $\alpha_7 = 1.02$ | $\alpha_7 = 1.01$ |
| $i=8$ | $\alpha_8 = 1.01$ | $\alpha_8 = 0.979$ | $\alpha_8 = 0.993$ |
| $i=9$ | $\alpha_9 = 0.979$ | $\alpha_9 = 0.970$ | $\alpha_9 = 0.985$ |
| $i=10$ | $\alpha_{10} = 1.06$ | $\alpha_{10} = 1.10$ | $\alpha_{10} = 1.14$ |
| $i=11$ | $\alpha_{11} = 1.14$ | $\alpha_{11} = 0.956$ | $\alpha_{11} = 1.15$ |
| $i=12$ | $\alpha_{12} = 1.01$ | $\alpha_{12} = 1.00$ | $\alpha_{12} = 1.01$ |
| $i=13$ | $\alpha_{13} = 1.01$ | $\alpha_{13} = 1.07$ | $\alpha_{13} = 1.04$ |

| | | | |
|--------|-----------------------|----------------------|----------------------|
| $i=14$ | $\alpha_{14} = 0.992$ | $\alpha_{14} = 1.21$ | $\alpha_{14} = 1.10$ |
| R^2 | 0.96 | 0.96 | 0.93 |

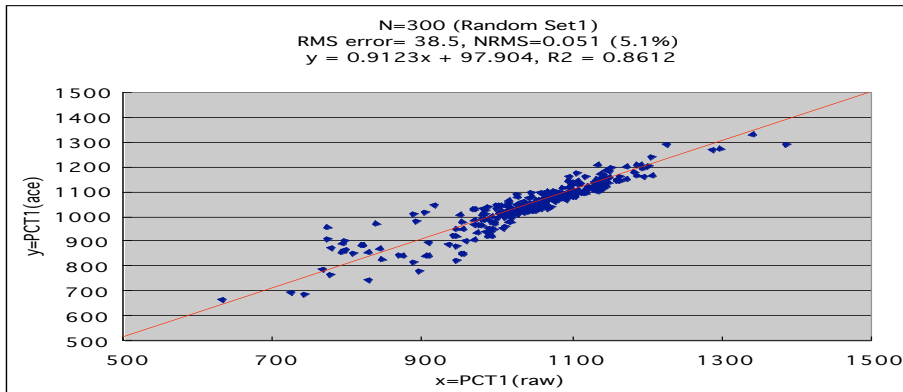
The three plots of transformed variables $\hat{\theta}^*(y)$ and $\hat{\phi}_i^*(x_i)$ in Figure 2 show approximate linearity with higher R^2 , explaining quite good approximations to $\theta^*(y)$ and $\phi_i^*(x_i)$ with the ACE algorithm. This results are also justified by the regression coefficients ($\alpha_i, i=1,2,\dots,p$) between $\hat{\phi}_i(x_i)$ and $\hat{\theta}(y)$ in Table 3, approaching 1 for most $\hat{\phi}^*(x_i)$.

On the other hand, the comparison with the original MARS results (Figures 3-4) explains that except for the lower PCT values (subject to highly nonlinear thermal-hydraulic behavior), the ACE-RSM Models relatively well trace the original MARS results, compared to the corresponding linear regression models (see Table 3). From the qualitative aspect, the ACE-RSM-Model-3 (based on a larger number of samples) is quickly converged to the original results, compared with ACE-RSM-Model-1 and Model-2 subject to higher values of R^2 . This fact indicates that although the RSM itself is well fitted to the original code results smaller number of samples may not trace the whole trend of the original MARS code results that are not explained due to their random variation. In order to cover such a random variation that may be not explained by the limited number of samples, it is better to employ appropriate number of samples. From the quantitative aspect, the accuracy bound for ACE- Model-3 is in between ΔT |MARS-ACE|=5K for 95% PCT and 20K for 5% PCT (e.g., see the case of N=3000 of Table 4). The above results indicate that the ACE-RSM models could give an appropriate surrogate model to the original MARS code, although they also show a greater or less dependency on the utilized number of samples as in the conventional RSM.



(a) ACE-Model-1: $R^2 = 0.9260$, Normalized RMS=0.037 (3.7%) (b) ACE-Model-2: $R^2 = 0.9257$, Normalized RMS=0.044 (4.4%)

Figure 3. Comparison with MARS result (ACE-RSM-1 and 2)



ACE-RSM-3: $R^2 = 0.8575$, Normalized RMS=0.056 (5.6%)

Figure 4. Comparison with MARS result (ACE-RSM-3)

Table 3. Linear regression coefficients between the original inputs and output.

| | | | | | |
|--|--|-----------------|---------------------|------------------------------|--------------------------|
| Coeff. of determination $R^2 = \frac{\sum_{j=1}^N (\hat{y}_j - \bar{y})^2}{\sum_{j=1}^N (y_j - \bar{y})^2}$ | Linear regression between original inputs and output $\hat{y} = \beta_0 + \sum_{i=1}^{p=14} \beta_i x_i$ | | | | |
| | 1 st order RSM | Rank regression | Partial correlation | Standardized rank regression | Partial rank correlation |
| R^2 (RSM-1) | 0.85 | 0.85 | 0.85 | 0.81 | 0.81 |
| R^2 (RSM-2) | 0.84 | 0.84 | 0.84 | 0.82 | 0.82 |
| R^2 (RSM-3) | 0.81 | 0.81 | 0.81 | 0.79 | 0.79 |

Table 4. 5/95% PCT (K) values for three ACE-RSM models.

| N | MARS | | ACE-RSM-1 ($R^2=0.9260$) | | ACE-RSM-2 ($R^2=0.9257$) | | ACE-RSM-3 ($R^2=0.8612$) | |
|-------|--------------|---------------|-------------------------------|---------------|-------------------------------|---------------|-------------------------------|---------------|
| | 5% | 95% | 5% | 95% | 5% | 95% | 5% | 95% |
| 124 | 790.0 | 1286.5 | 824.3 | 1200.8 | 846.1 | 1212.0 | 794.0 | 1204.8 |
| 300 | 817.7 | 1171.3 | 884.8 | 1189.5 | 886.9 | 1178.5 | 852.6 | 1182.2 |
| 500 | 805.8 | 1172.1 | 881.7 | 1182.6 | 883.0 | 1176.6 | 846.7 | 1173.4 |
| 1000 | 810.7 | 1173.5 | 864.8 | 1181.4 | 867.7 | 1177.4 | 835.0 | 1173.7 |
| 3000 | 815.5 | 1174.4 | 861.2 | 1179.0 | 867.8 | 1177.7 | 834.4 | 1176.0 |
| 6000 | - | - | 859.3 | 1179.3 | 867.5 | 1178.6 | 834.8 | 1177.1 |
| 9000 | - | - | 857.5 | 1179.0 | 864.8 | 1178.6 | N/A | - |
| 10000 | - | - | 857.4 | 1178.6 | 864.5 | 1178.6 | N/A | - |

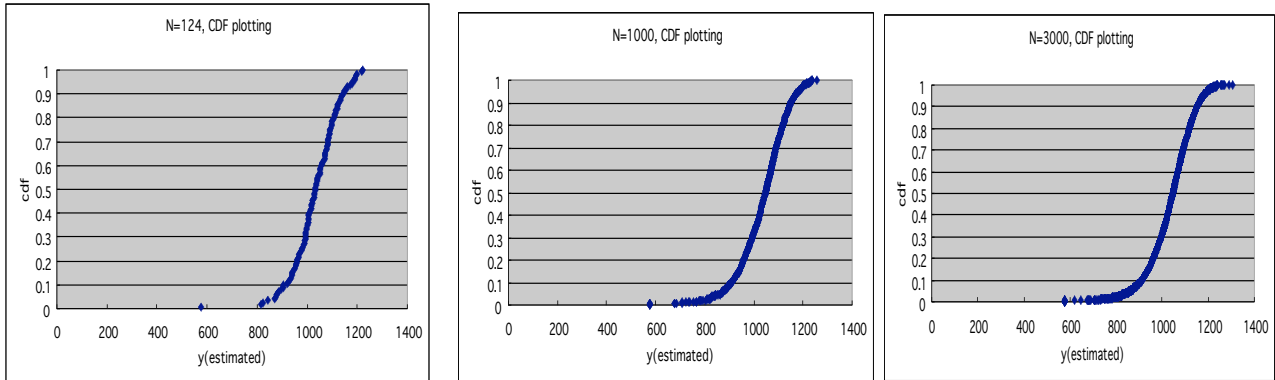


Figure 5. CDF variation according to the increase of sample N (based on ACE-RSM-1)

6 CONCLUSION

The ACE-RSM approach has been applied to assess the blowdown PCT uncertainty for the LOFT L2-5 Experiment as a complementary work to the OECD BEMUSE Phase-III program. A comparison with the original code results shows that except for the lower PCT values (subject to highly nonlinear thermal-hydraulic behaviour), the formulated ACE-RSM Models relatively well trace the original code results, even with a limited number of code runs. Since the aforementioned nonlinear thermal-hydraulic behaviour highly depends on a physical domain of a system rather than a random error, its impact on the final results should be explained by the other means in more detail (e.g., physical models employed in the thermal-hydraulic system code).

On the other hand, a greater or lesser dependency on the utilized number of samples could be reduced further by employing more efficient sampling schemes like the Latin Hypercube Sampling (LHS) approach [McKay et al., 1979; Iman et al., 1984]. More specifically, the LHS approach provides much less dependency on the size of statistical samples than random sampling and suitable for the approximation of computer experiments, which mainly have system error rather than random error. However, they have not been taken into account in the present analysis since there are no currently available LHS results through the original code.

Acknowledgements. This work was supported by Nuclear Research & Development Program of the Korea Science and Engineering Foundation (KOSEF) grant funded by the Korean government (MEST).

REFERENCES

- Breiman L., and Friedman, J.H. 1985. Estimating optimal transformations for multiple regression and correlation, *Journal of American Statistical Association*, Vol. 80, p.580-598.
- Chung, B. D. 2005. Uncertainty quantification of LOFT L2-5 experiment, presented in OECD/NEA BEMUSE phase III activity 3rd meeting, October 26-28, Grenoble, France.
- Cleveland, W. S. 1979. Robust locally weighted regression and smoothing scatterplots, *Journal of American Statistical Association*, Vol. 74, p.828-836.
- Crécy, A., and Bazin, P. 2007. BEMUSE phase III report: uncertainty and sensitivity analysis of the LOFT L2-5 test, CEA, France.
- Glaeser, H. 2000. Uncertainty evaluation of thermal-hydraulic code results, International Meeting on "Best-Estimate" Methods in Nuclear Installation Safety Analysis (BE-2000), Washington, DC, November.
- Helton, J. C. and Davis, F. J. 2002. Illustration of Sampling-Based Methods for Uncertainty and Sensitivity Analysis, *Risk Analysis*, Vol. 22: 3, p.591-622.
- Iman, R. L., and Shortencarier, M. J. 1984. A fortran 77 program and user's guide for the generation of Latin Hypercube and Random Samples for use with computer models, NUREG/CR-3624, Technical Report SAND83-2365, Sandia National Laboratories, Albuquerque, NM.
- IAEA, 2008. Best estimate safety analysis for nuclear power plants: uncertainty evaluation, IAEA Safety Reports Series No.52, Vienna, Austria.
- Nutt, W. T. and Wallis, G. B. 2004. Evaluation of nuclear safety from the outputs of computer codes, *Reliability Engineering and System Safety*, Vol.83, p.57-77.
- Wang, D. and Murphy, M. 2005. Identifying Nonlinear Relationships in Regression using the ACE Algorithm, *Journal of Applied Statistics*, Vol. 32:3, p.243-258.
- McKay, M. D., Bechman, R. J., and Conover, W. J. 1979. A comparison of three methods for selecting values of input variables in the analysis of output from a computer code, *Technometrics*, Vol. 21:2, p.239-245.
- Sacks, J., Welch, W. J., Mitchell, T. J., and Wynn, H. P. 1989. Design and analysis of computer experiments, *Statistical Science*, Vol. 4:4, p. 409-435.
- Wilks, S. S. 1941. Determination of sample sizes for setting tolerance limits, *The Annals of Mathematical Statistics*, Vol.12, p.91-96.